The timing diagram for the first several cycles of the generation of the sub-transform $u$ is given in Table 1, where the boldfaced expressions denote the exceptional operation of the corresponding multiplexers, e.g. in normal conditions, multiplexer MUX1 selects the upper input and feeds the output to PE1. In exceptional conditions when $T = 6 + 8k$ (with integer $k$), the lower input of MUX1 is selected. The control signal to MUX1 comes from a tag attached to the first signal component $x1$. Similarly, the multiplexer MUX3 selects the upper input in normal conditions except at $T = 10 + 8k$, when the lower input is selected. Again, the control signal to MUX3 comes from a tag attached to the input signal $x8$.

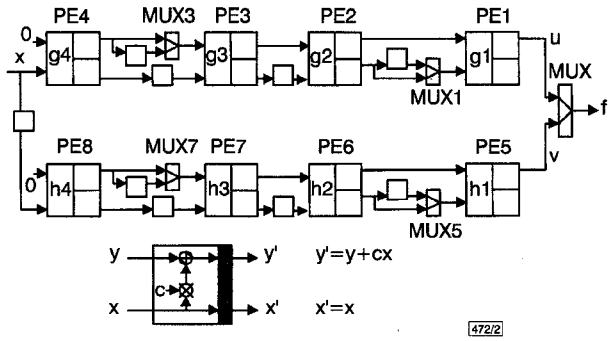


**Fig. 2** *VLSI architecture for even-size W-transform*

Similarly, another half transform $v = H_{4,8}x$ is realised by the lower part of the architecture in Fig. 2 with PE5 to PE8. The operations of the $H$ part are the same as those for the $G$ part except for one additional delay register in the input signal. Each sample of the final W-transform output $f$ comes from either one of $u$ or $v$, determined by the appended multiplexer MUX which selects the output from the $G$ part and the $H$ part in turns every other cycle. In other words, the first transform output $f1 = u1$ is generated at cycle six; the second transform output $f2 = v1$ is generated at cycle 7; $f3 = u2$ is generated at cycle eight; $f4 = v2$ is generated at cycle nine, ... etc.

The odd-size W-transform is defined in a similar way to eqn. 1, except for some irregular entries in the last rows of $G$ and $H$ [3]. Furthermore, the coefficient matrix pair $G'$ and $H'$ of the inverse W-transform has a similar structure to that of the forward transform. Hence, both the forward and inverse W-transforms of arbitrary size can be realised on a unified architecture similar to Fig. 2 by properly arranging the position of the multiplexers inserted between the PEs.

**Table 1:** Timing diagram for PE1 to PE4 in Fig. 2 for even-size W-transform processor

| T | PE4 | PE3 | PE2 | PE1 |
|---|---|---|---|---|
| 1 | | | | |
| 2 | | | | |
| 3 | $g4x3$ | | | |
| 4 | $g4x4$ | $g4x3+g3x2$ | | |
| 5 | $g4x5$ | $g4x4+g3x3$ | $g4x3+g3x2+g2x1$ | |
| 6 | $g4x6$ | $g4x5+g3x4$ | $g4x4+g3x3+g2x2$ | **$g4x3+g3x2+g2x1+g1x1$ ($u1$)** |
| 7 | $g4x7$ | $g4x6+g3x5$ | $g4x5+g3x4+g2x3$ | $g4x4+g3x3+g2x2+g1x1$ |
| 8 | $g4x8$ | $g4x7+g3x6$ | $g4x6+g3x5+g2x4$ | $g4x5+g3x4+g2x3+g1x2$ ($u2$) |
| 9 | $g4x'1$ | $g4x8+g3x7$ | $g4x7+g3x6+g2x5$ | $g4x6+g3x5+g2x4+g1x3$ |
| 10 | $g4x'2$ | **$g4x8+g3x8$** | $g4x8+g3x7+g2x6$ | $g4x7+g3x6+g2x5+g1x4$ ($u3$) |
| 11 | $g4x'3$ | $g4x'2+g3x'1$ | $g4x8+g3x8+g2x7$ | $g4x8+g3x7+g2x6+g1x5$ |
| 12 | $g4x'4$ | $g4x'3+g3x'2$ | $g4x'2+g3x'1+g2x8$ | $g4x8+g3x8+g2x7+g1x6$ ($u4$) |
| 13 | $g4x'5$ | $g4x'4+g3x'3$ | $g4x'3+g3x'2+g2x'1$ | $g4x'2+g3x'1+g2x8+g1x7$ |
| 14 | $g4x'6$ | $g4x'5+g3x'4$ | $g4x'4+g3x'3+g2x'2$ | **$g4x'3+g3x'2+g2x'1+g1x'1$ ($u'1$)** |
| 15 | $g4x'7$ | $g4x'6+g3x'5$ | $g4x'5+g3x'4+g2x'3$ | $g4x'4+g3x'3+g2x'2+g1x'1$ |
| 16 | $g4x'8$ | $g4x'7+g3x'6$ | $g4x'6+g3x'5+g2x'4$ | $g4x'5+g3x'4+g2x'3+g1x'2$ ($u'2$) |

VLSI implementation of a W-transform processor is completed using the standard cell design method with a 0.6μm cell library. The processor is intended to be used as the core part in W-transform-based systems for multi-resolution image processing since it can compute 1D W-transforms of arbitrary length (both even- and odd-lengths). Table 2 gives the chip information for the design. The processor, occupying only a very small hardware area, can operate at a frequency of up to 90MHz, and thus is sufficient for most real-time image processing applications; e.g. it takes only 5.8ms for this processor to perform a 2D W-transform on a 512 × 512 image with 256 grey levels for each pixel. Note that a higher throughput rate can easily be achieved if we further pipeline the multiplication-addition in each PE.

**Table 2:** Chip information for W-transform processor based on a 0.6μm cell library

| Function | W-transform of arbitrary size |
|---|---|
| Bit accuracy | 8 bit (256 grey levels) |
| Cycle time [ns] | 11.2 |
| Core area [μm²] | 1500 × 1550 |
| Gate count | 4336 |

*Conclusion:* We have demonstrated VLSI implementation of the W-transform which can be used to speed up W-transform-based multi-resolution image processing, including image compression and analysis. The regular architecture of the processor is fully pipelined with a high-throughput rate and low hardware cost, and can computer a W-transform for any size of signals.


*13 November 1997*
*Electronics Letters Online No: 19980206*

Shen-Fu Hsiao (*Institute of Computer and Information Engineering, National Sun Yat-Sen University, Taiwan, Republic of China*)

E-mail: sfhsiao@cie.nsysu.edu.tw

**References**

1 MALLAT, S.G.: 'A theory for multi-resolution signal decomposition: The wavelet representation', *IEEE Trans. Pattern Anal. Mach. Intell.*, 1989, **PAMI-11**, (7), pp. 674–693
2 ANTONINI, M.: 'Image coding using wavelet transform', *IEEE Trans. Signal Process.*, 1992, **1**, (2), pp. 205–220
3 KWONG, M.K., and TANG, P.T.: 'W-matrices and non-orthogonal multi-resolution analysis of finite signals of arbitrary length'. Mathematics and Computer Science Division Preprint MCS-P449-0794, Argonne National Lab., 1994
4 KWONG, M.K., and LIN, B.: 'W-transform method for feature-oriented multiresolution image retrieval'. Proc. SPIE: Wavelet Applications II, April 1995, Vol. 2491, pp. 1086–1095
5 REYNOLDS, W.D.: 'Image compression using W-Transform'. Mathematics and Computer Science Division Reprint Series MCS-P524-0894, Argonne National Lab., 1994
6 DAUBECHIES, I.: 'Ten lectures on wavelets'. SIAM, Philadelphia, Pennsylvania, 1992

## Noncoherent sequence detection of CPM

G. Colavolpe and R. Raheli

Schemes in which noncoherent sequence detection based on the Viterbi algorithm are proposed for linearly modulated signals transmitted over additive white Gaussian noise channels, have recently been proposed by the authors. These schemes are attractive because their performance closely approaches that of coherent receivers with acceptable complexity, and they avoid the drawbacks of phase-locked loops. The authors extend these results to $M$-ary continuous phase modulation (CPM) signals.

*Introduction:* We have recently proposed noncoherent sequence detection for linearly modulated signals transmitted over additive white Gaussian noise channels [1, 2], and now extend these results to $M$-ary continuous phase modulation (CPM) signals. The schemes are based on the Viterbi algorithm.

*Proposed algorithm:* The complex envelope of CPM signals has the form

$$s(t,\underline{\alpha}) = \exp\left\{ j2\pi h \sum_{n=0}^{\infty} \alpha_n q(t-nT) \right\} \qquad (1)$$

in which $T$ is the signalling interval, $h$ is the modulation index, the information symbols $\{\alpha_n\}_{n=0}^{\infty}$ are independent and take on values in the $M$-ary alphabet $\{\pm1, \pm3, ..., \pm(M-1)\}$ with equal probability; and $\underline{\alpha} \triangleq (\alpha_0, \alpha_1, ..., \alpha_n, ...)$ denotes the information sequence. The function $q(t)$ is the phase smoothing response.

Based on Laurent decomposition [3], the complex envelope of $M$-ary CPM signals may be exactly expressed as

$$s(t,\underline{\alpha}) = \sum_{k=0}^{K-1} \sum_{n} a_{k,n} h_k(t-nT) \qquad (2)$$

The number $K$ of linearly modulated components, and the expressions of the pulses $\{h_k(t)\}$ and the symbols $\{a_{k,n}\}$ as a function of the information symbol sequence $\{\alpha_n\}$, may be found in [3]. If $M$ is a power of two, most of the signal power is concentrated in the first $M-1$ components [3]. As a consequence, a value of $K = M-1$ may be used in eqn. 2 to attain a very good trade-off between approximation quality and number of signal components.

The complex envelope of the received signal may be modelled as:

$$r(t) = s(t,\underline{\alpha})e^{j\theta} + w(t) \qquad (3)$$

where $w(t)$ is a complex-valued Gaussian white noise process with independent components, each with two-sided power spectral density $N_0$, and $\theta$ is an unknown constant phase shift introduced by the channel.

The sampled output of a set of filters matched to the pulses of the Laurent representation may easily be shown to be sufficient statistics for optimal non-coherent detection of the information sequence. Assuming perfect knowledge of symbol timing, the output, sampled at time $nT$, of a filter matched to the pulse $h_k(t)$ may be expressed as

$$x_{k,n} \triangleq r(t) \otimes h_k(-t)\big|_{t=nT} = y_{k,n}e^{j\theta} + n_{k,n} \qquad (4)$$

where $y_{k,n}$ and $n_{k,n}$ are the signal and noise components, and $\otimes$ denotes convolution. It is easy to show that $y_{k,n} \neq a_{k,n}$ because of inter-symbol interference (ISI) and interference from other signal components. The noise terms are characterised by the following cross-correlation function:

$$E\{n_m(t)n_k^*(t-\tau)\} = 2N_0\rho_{m,k}(-\tau) \qquad (5)$$

which depends on the shape of pulses $\rho_{m,k}(t) \triangleq h_m(t) \otimes h_k(-t)$.

A coherent receiver, based on Laurent decomposition, processes this sampled output using a Viterbi algorithm with branch metrics [4]

$$\lambda_n \triangleq \mathrm{Re}\left\{ e^{-j\theta} \sum_{k=0}^{K-1} x_{k,n}\tilde{a}_{k,n}^*(\underline{\tilde{\alpha}}) \right\} \qquad (6)$$

where $\underline{\tilde{\alpha}}$ is a hypothetical information sequence. The performance of this simplified coherent receiver is practically equal to that of the optimal coherent receiver [4]. The proposed noncoherent sequence detection scheme is based on the concept of estimating the phase $\theta$ using the sampled output of a few matched filters. This estimation takes into account both ISI and noise correlation. Specifically, at time instant $nT$ we use: the sampled outputs of the first $k_1$ matched filters at time $(n-1)T$, those of the first $k_2$ matched filters at time $(n-2)T$ and so on until those of the first $k_{N-1}$ filters at time $(n-N+1)T$, where $N$ is an integer. It is convenient to denote by $\mathbf{x}_n$ a vector which collects these sampled outputs, and define $\mathbf{k} \triangleq (k_1, k_2, ..., k_{N-1})$. Adopting similar definitions for the signal and noise components of $\mathbf{x}_n$, we may write eqn. 4 in the form $\mathbf{x}_n = \mathbf{y}_n e^{j\theta} + \mathbf{n}_n$. It is easy to verify that the data-aided ML estimator of the unknown phase is such that

$$e^{-j\hat{\theta}} = \frac{\mathbf{x}_n^{*T}\mathbf{C}^{-1}\mathbf{y}_n}{|\mathbf{x}_n^{*T}\mathbf{C}^{-1}\mathbf{y}_n|} \qquad (7)$$

where $\mathbf{C} \triangleq E\{\mathbf{n}\mathbf{n}^{*T}\}$ is the noise covariance matrix.

To derive a noncoherent detection scheme, we proceed by replacing the unknown phasor $e^{-j\theta}$ in eqn. 6 with the estimator in eqn. 7. To circumvent the need for the data-aiding sequence, which affects vector $\mathbf{y}_n$, per-survivor processing (PSP) is adopted [5]. Specifically, a PSP-based estimate $\hat{\theta}(\underline{\tilde{\alpha}})$ may be defined according to

$$e^{-j\hat{\theta}(\underline{\tilde{\alpha}})} = \frac{\mathbf{x}_n^{*T}\mathbf{C}^{-1}\mathbf{y}_n(\underline{\tilde{\alpha}})}{|\mathbf{x}_n^{*T}\mathbf{C}^{-1}\mathbf{y}_n(\underline{\tilde{\alpha}})|} \qquad (8)$$

where the dependence of $\mathbf{y}_n(\underline{\tilde{\alpha}})$ from the hypothetical information sequence $\underline{\tilde{\alpha}}$ has been emphasised.

Replacing eqn. 8 into eqn. 6 and neglecting the denominator $|\mathbf{x}_n^{*T}\mathbf{C}^{-1}\mathbf{y}_n(\underline{\tilde{\alpha}})|$ in order to simplify the metrics, we obtain the following branch metrics

$$\lambda_n = \mathrm{Re}\left\{ \sum_{k=0}^{K-1} x_{k,n}\tilde{a}_{k,n}^*(\underline{\tilde{\alpha}}) \left[\mathbf{x}_n^{*T}\mathbf{C}^{-1}\mathbf{y}_n(\underline{\tilde{\alpha}})\right] \right\} \qquad (9)$$

These branch metrics may be expressed as functions of the information symbols $\alpha_n$. Owing to the dependence of these branch metrics on the sampled matched filter output through products of the type $x_{k,n}x_{l,n-i}^*$ only, the proposed detection scheme is inherently noncoherent. The branch metrics in eqn. 9 may be rearranged as

$$\lambda_n = \mathrm{Re}\left\{ \sum_{k=0}^{K-1} x_{k,n}\left[\mathbf{x}_n^{*T}\mathbf{C}^{-1}\mathbf{f}_k(\underline{\tilde{\alpha}})\right] \right\} \qquad (10)$$

where $\mathbf{f}_k(\underline{\tilde{\alpha}}) \triangleq \tilde{a}_{k,n}^*(\underline{\tilde{\alpha}})\mathbf{y}_n(\underline{\tilde{\alpha}})$ is the only data dependent factor. It is worth noting that the vector $\mathbf{C}^{-1}\mathbf{f}_k(\underline{\tilde{\alpha}})$ may be precomputed for each trellis branch.

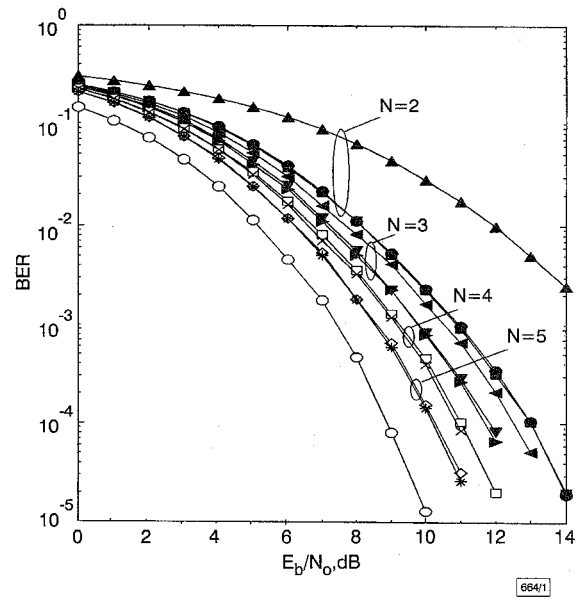


**Fig. 1** *GMSK modulation with BT = 0.25*

▲ $S = 4$, $N = 2$ and $\mathbf{k} = 1$
■ $S = 4$, $N = 2$ and $\mathbf{k} = 2$
● $S = 8$, $N = 2$ and $\mathbf{k} = 2$
◀ $S = 8$, $N = 3$ and $\mathbf{k} = (1, 1)$
▼ $S = 8$, $N = 3$ and $\mathbf{k} = (2, 1)$
▶ $S = 8$, $N = 3$ and $\mathbf{k} = (2, 2)$
□ $S = 8$, $N = 4$ and $\mathbf{k} = (1, 1, 1)$
× $S = 16$, $N = 4$ and $\mathbf{k} = (1, 1, 1)$
◇ $S = 16$, $N = 5$ and $\mathbf{k} = (1, 1, 1, 1)$
✳ $S = 32$, $N = 5$ and $\mathbf{k} = (1, 1, 1, 1)$
○ optimal coherent receiver

The number of trellis states depends on $N$ and the length of pulses $\rho_{m,k}(t)$, and does not depend on the number of matched filters, i.e. on the entries of vector $\mathbf{k}$. However, this number of states may be limited by reduced-state sequence detection, RSSD (see [5] and its references). As a consequence, integer $N$ and the number of trellis states $S$ play the role of two independent parameters which control the receiver complexity.

Integer $N$ affects the number of previous symbols which aid an implicit per-survivor phase estimator. We refer to $N$ as the 'implicit phase memory'. Intuitively a better phase estimate is obtained using a larger value of $N$, and at the limit where $N \to +\infty$ coherent detection performance is obtained. Moreover, even using small values of $N$ (a few units) a performance very close to that of coherent detection may be achieved, as shown in the next Section. On the other hand, under dynamic channel conditions, receivers with an $N$ of a few units have a robustness to phase jitter, and frequency offsets similar to those of differential detectors.

*Numerical results and discussion:* We have analysed the performance of the proposed noncoherent detection schemes by computer simulation for Gaussian minimum shift keying (GMSK), with a parameter $BT$ set to 0.25 and a quaternary 2RC modulation,

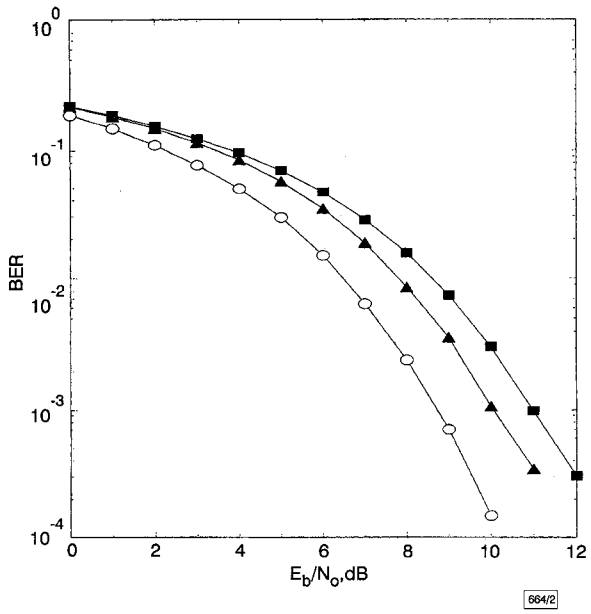


**Fig. 2** *Quaternary 2RC modulation with h = 0.25*

▲ $N = 4$, $S = 64$, $\mathbf{k} = (3, 1, 1)$
■ $N = 3$, $S = 16$ and $\mathbf{k} = (3, 1)$
○ optimal coherent receiver

(raised-cosine frequency pulse with a duration of two symbol intervals) and a modulation index $h = 0.25$. The resulting performance is shown in Figs. 1 and 2 for receivers with various degrees of complexity, in terms of bit error rate (BER) against $E_b/N_0$, $E_b$ being the received signal energy per information bit. The performance of the optimal coherent receiver is also shown for comparison. A general conclusion which can be drawn from the Figures is that the performance improves with increasing receiver complexity and approaches that of optimal coherent detection. Receiver complexity is defined here in terms of: (i) implicit phase memory $N$; (ii) the number $S$ of trellis states; (iii) the number of matched filter outputs, i.e. the number of entries of vector $\mathbf{k}$. For a fixed value of $N$, we may observe that the performance greatly improves if the phase estimate uses not only the output of the first matched filter $h_0(-t)$ but also that of the other matched filters.

*Acknowledgments:* This work was performed within a research cooperation between Dipartimento di Ingegneria dell'Informazione, Università di Parma, Italy and Italtel S.p.A., Milano, Italy.


*2 November 1997*
*Electronics Letters Online No: 19980225*

G. Colavolpe and R. Raheli (*Dipartimento di Ingegneria dell'Informazione, Università di Parma, Viale delle Scienze, 43100 Parma, Italy*)

E-mail: raheli@tlc.unipr.it

### References

1 COLAVOLPE, G., and RAHELI, R.: 'Non-coherent sequence detection of M-ary PSK'. IEEE Int. Conf. Commun. (ICC'97), Montreal, Canada, 1997, pp. 21–25
2 COLAVOLPE, G., and RAHELI, R.: 'Non-coherent sequence detection of QAM'. IEEE Int. Symp. Inform. Theory (ISIT'97), Ulm, Germany, 1997, pp. 536
3 MENGALI, U., and MORELLI, M.: 'Decomposition of M-ary CPM signals into PAM waveforms', *IEEE Trans. Inf. Theory*, 1995, **41**, pp. 1265–1275
4 COLAVOLPE, G., and RAHELI, R.: 'Reduced-complexity detection and phase synchronization of CPM signals', *IEEE Trans. Commun.*, 1997, **45**, pp. 1070–1079
5 RAHELI, R., POLYDOROS, A., and TZOU, C.K.: 'Per-survivor processing: a general approach to MLSE in uncertain environments', *IEEE Trans. Commun.*, 1995, **43**, pp. 354–364

## Use of fast Walsh-Hadamard transformation for optimal symbol-by-symbol binary block-code decoding

L.E. Nazarov and V.M. Smolyaninov

A procedure for optimal symbol-by-symbol binary block-code decoding is presented: it uses the spectral Walsh-Hadamard transformation. The dimension of the Walsh-Hadamard basis is equal to that of dual codes. The realisation of the described procedure, using the fast Walsh-Hadamard transformation application, is seen to be the most efficient in terms of computational complexity for high-rate code decoding, in comparison with known symbol-by-symbol decoding procedures.

*Introduction:* The problem of computationally efficient decoding algorithm searching is of great interest at present. The decoding algorithms can be separated into two general families according to the realisation of the decoding rule: maximum-likelihood decoding methods which minimise the probability of word error, and decoding methods which minimise the symbol error probability.

The foundation of the first decoding algorithm family is the Viterbi algorithm [1], where the decoding complexity is determined by the code trellis structure [2 – 6]. Another maximum-likelihood decoding algorithm is found by applying the fast Walsh-Hadamard transformation (FHT). This is advantageous for low-rate codes; those algorithms concerned with the particular structure of a code generator matrix are an attractive alternative to Viterbi decoding for some codes [7 – 11].

The procedures used in the second decoding algorithm family form the basis of the iterative decoding of perspective codes (turbo-codes [12, 13], product-codes [13]). In [14], the optimal decoding algorithm minimising symbol error rate (MAP) has been derived. This algorithm consists of two recursive relations. The suboptimal symbol-by-symbol decoding algorithm (SOVA) [13] is less complicated than the computational complexity of the MAP. The SOVA is the Viterbi algorithm in MAP form, and therefore the SOVA and Viterbi algorithms have the same decoding complexity. The block-codes can also be decoded using MAP and SOVA, owing to the their trellis structure [3].

There is another known optimum decoding algorithm minimising the symbol error probability for block-codes [15]. This algorithm uses dual codes, and therefore it is attractive for high-rate codes. The possibility of realisisng this algorithm with the FHT application is shown in this Letter. The decoding complexities of the derived procedure and of the known decoding procedures are compared, and it is shown that the decoding procedure described in this Letter is the most computationally efficient for high-rate codes (e.g. Hamming codes).

*General problem:* Let $A = (a_i;\ 0 \le i < k)$ denote the information symbols $a_i$ for the $(n,k)$ codeword $B = (b_l;\ 0 \le l < n)$; $H = (h_{ml};\ 0 \le m < n-k,\ 0 \le l < n)$ denote the generator matrix of the dual code $(n, n-k)$ and $Y = (y_l(t);\ 0 \le l < n)$ denote the received word. The likelihood function $p\{Y|B\}$ is believed to be known. Given $Y$, the decoding problem is to compute *a posteriori* probability $Pr\{b_l|Y\}$ for $b_l$. If the code is systematic, this rule minimises the probability of information symbol error. In the following we describe the procedure for realising this rule by means of a Walsh-Hadamard Transformation (WHT) application.

As in [15], we use a memoryless channel, the vectors $A$ being equiprobable. The optimum symbol-by-symbol decoding algorithm derived in [15] can be rewritten taking into account the normalisation as

$$C(l) = \Pr\{b_l = 0|Y\} - \Pr\{b_l = 1|Y\} = \frac{1}{\sum_{v=0}^{2^{n-k}-1} D_v} \sum_{v=0}^{2^{n-k}} D_v \cdot \lambda_l(v) \quad (1)$$

where

$$\lambda_l(v) = \begin{cases} \rho_l & t_v(l) = 0 \\ \frac{1}{\rho_l} & t_v(l) = 1 \end{cases} \quad (2)$$

$$\rho_l = \frac{p\{y_l(t)|b_l = 0\} - p\{y_l(t)|b_l = 1\}}{p\{y_l(t)|b_l = 0\} + p\{y_l(t)|b_l = 1\}} \quad (3)$$